

AD-A044 245

AEROSPACE CORP EL SEGUNDO CALIF AEROPHYSICS LAB
SENSITIVE F2 ABSORPTION DIAGNOSTIC.(U)
AUG 77 D J SPENCER

F/G 20/5

UNCLASSIFIED

TR-0077(2610)-3

SAMSO-TR-77-191

F04701-76-C-0077
NL

| OF |

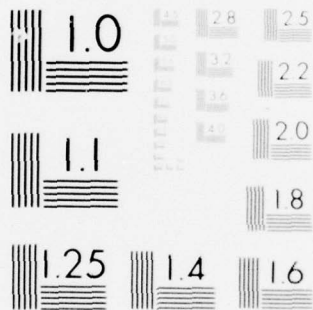
AD
A044245



END
DATE
FILMED

10 -77

DDC



MICROCOPY RESOLUTION TEST CHART
NATIONAL BUREAU OF STANDARDS-1963-A

AD A044245

12
B.S.

Sensitive F₂ Absorption Diagnostic

Aerophysics Laboratory
The Ivan A. Getting Laboratories
The Aerospace Corporation
El Segundo, Calif. 90245

15 August 1977

Interim Report

APPROVED FOR PUBLIC RELEASE:
DISTRIBUTION UNLIMITED

Prepared for

AIR FORCE WEAPONS LABORATORY
Kirtland Air Force Base, N.Mex. 87117

SPACE AND MISSILE SYSTEMS ORGANIZATION
AIR FORCE SYSTEMS COMMAND
Los Angeles Air Force Station
P.O. Box 92960, Worldway Postal Center
Los Angeles, Calif. 90009

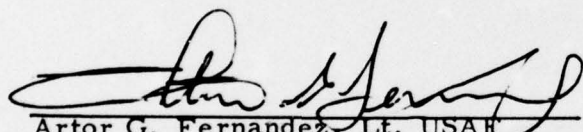
AD No. _____
DDC FILE COPY

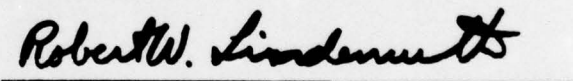
DDC
RECEIVED
SEP 19 1977
B

This interim report was submitted by The Aerospace Corporation, El Segundo, CA 90245, under Contract No. F04701-76-C-0077 with the Space and Missile Systems Organization, Deputy for Advanced Space Programs, P.O. Box 92960, Worldway Postal Center, Los Angeles, CA 90009. It was reviewed and approved for The Aerospace Corporation by W. R. Warren, Jr., Aerophysics Laboratory. Lieutenant A. G. Fernandez, SAMSO/YAPT, was the project officer for Advanced Space Programs.

This report whas been reviewed by the Information Office (OI) and is releasable to the National Technical Information Service (NTIS). At NTIS, it will be available to the general public, including foreign nations.

This technical report has been reviewed and is approved for publication. Publication of this report does not constitute Air Force approval of the report's findings or conclusions. It is published only for the exchange and stimulation of ideas.


Artor G. Fernandez, Lt, USAF
Project Officer


Robert W. Lindemuth, Lt Col, USAF

FOR THE COMMANDER


Floyd R. Stuart, Colonel, USAF
Deputy for Advanced Space Programs

UNCLASSIFIED

SECURITY CLASSIFICATION OF THIS PAGE (When Data Entered)

REPORT DOCUMENTATION PAGE		READ INSTRUCTIONS BEFORE COMPLETING FORM
1. REPORT NUMBER SAMSO-TR-77-191	2. GOVT ACCESSION NO.	3. RECIPIENT'S CATALOG NUMBER
4. TITLE (and Subtitle) SENSITIVE F ₂ ABSORPTION DIAGNOSTIC	5. TYPE OF REPORT & PERIOD COVERED Interim + Rept.	6. PERFORMING ORG. REPORT NUMBER TR-0077(2610)-3
7. AUTHOR(s) Donald J. Spencer	8. CONTRACT OR GRANT NUMBER(s) F04701-76-C-0077	
9. PERFORMING ORGANIZATION NAME AND ADDRESS The Aerospace Corporation El Segundo, Calif. 90245	10. PROGRAM ELEMENT, PROJECT, TASK AREA & WORK UNIT NUMBERS	
11. CONTROLLING OFFICE NAME AND ADDRESS Air Force Weapons Laboratory Kirtland Air Force Base, N. Mex. 87117	12. REPORT DATE 15 Aug 1977	13. NUMBER OF PAGES 24
14. MONITORING AGENCY NAME & ADDRESS (if different from Controlling Office) Space and Missile Systems Organization Air Force Systems Command Los Angeles, Calif. 90009	15. SECURITY CLASS. (of this report) Unclassified	15a. DECLASSIFICATION/DOWNGRADING SCHEDULE
16. DISTRIBUTION STATEMENT (of this Report) Approved for public release; distribution unlimited 12 24 p.		
17. DISTRIBUTION STATEMENT (of the abstract entered in Block 20, if different from Report) DDC RECEIVED SEP 19 1977 RECEIVED B		
18. SUPPLEMENTARY NOTES		
19. KEY WORDS (Continue on reverse side if necessary and identify by block number) F ₂ Absorption, Nozzle Recombination Absorption Measurement Chemical Laser F ₂ Measurement delta sub d .0001		
20. ABSTRACT (Continue on reverse side if necessary and identify by block number) A sensitive F ₂ absorption diagnostic technique was developed by which a difference in absorption sensitivity of $\Delta I/I_0 = 10^{-4}$ can be determined. This value corresponds to an F ₂ pressure path length product of 0.215 Torr cm at 300 K. The method was applied to an HF(DF) chemical laser flow and resulted in measured average nozzle-exit values (α) of from 0.4 to 0.5 from a totally dissociated plenum, indicating a large degree of nozzle wall recombination. alpha		

DD FORM 1473
(FACSIMILE)

UNCLASSIFIED

SECURITY CLASSIFICATION OF THIS PAGE (When Data Entered)

409367

16

PREFACE

The assistance of James A. Beggs, Robert E. Cook, Marquis E. Gerard, Terry L. Felker, John M. Herbelin, and Robert R. Giedt in the operation of the arc-heated chemical laser facility is gratefully acknowledged. The assistance of Donald A. Durran and the use of his cold-flow facility for F_2 calibration were essential. The electronics expertise of David H. Ross and Munson A. Kwok is sincerely appreciated. The author also wishes to thank H. Mirels and Walter R. Warren, Jr., for encouragement in this project.

ACCESSION for	
NTIS	White Section <input checked="" type="checkbox"/>
DDC	Black Section <input type="checkbox"/>
UNANNOUNCED	<input type="checkbox"/>
JUSTIFICATION	
BY	
DISTRIBUTION/AVAILABILITY CODES	
Dist.	or SPECIAL
A	-

CONTENTS

PREFACE	1
I. INTRODUCTION.....	7
II. METHOD	9
III. CALIBRATION.....	17
IV. EXPERIMENTAL RESULTS.....	21
V. CONCLUDING REMARKS.....	27
REFERENCES.....	29

FIGURES

1.	Sensitive F_2 absorption experiment schematic.	10
2.	F_2 absorption device scope traces	13
3.	Theoretical calculation of temperature effect on F_2 continuum absorption coefficient at 325 nm	18
4.	F_2 absorption calibration in cold-flow facility	19
5.	F_2 density ratio measurement versus temperature.	24
6.	F_2 absorption measurements in SF_6 flow	26

I. INTRODUCTION

Uncertainties in the F-atom concentrations in the cavity flow region of cw HF and DF chemical lasers have hampered chemical efficiency calculations and plagued analytical attempts to model this type laser since its inception in 1969 [1,2]. F-atom uncertainties in the cavity region arise both as a result of uncertainties in F-atom concentrations in the plenum (resulting from temperature uncertainty and nonequilibrium chemistry effects) and uncertainties introduced by wall recombination of F atoms in the expansion nozzles [3,4]. This situation exists for both arc-heated and combustor-heated chemical lasers.

A technique was developed to measure average F_2 concentrations along a line in the nozzle flows from which the average F-atom concentration could be calculated for conditions of known total F_2 flow.

II. METHOD

In this method, simple absorption by the F_2 continuum was used to determine F_2 concentration. Previous work in the area of differential F_2 absorption measurement was performed by Suchard and Bergerson [5]. The current method was demonstrated and applied in the determination of the average F_2 concentration in the arc-heated flow of a standard 36-slit, cw, HF(DF) chemical laser MESA nozzle. A Liconix Model 301M HeCd modulatable laser operating at 325 nm was employed to probe the flow. The difference between the probe-beam and reference-beam intensities was measured with two independent silicon photovoltaic detectors and displayed on an oscilloscope for F_2 in the flow and no F_2 in the flow. A sensitivity of $\Delta I/I_0 = 10^{-4}$ was measured, which corresponds to a pressure-path length product of 0.215 Torr cm at 300 K.

Figure 1 is a schematic of the F_2 absorption experiment. The Liconix laser is square-wave modulated at ~ 20 Hz by an Interstate Electronics Model P25 pulse generator. The acousto-optic, intracavity modulation employed in this laser is essential to eliminate differential transients that are generated when mechanical choppers are employed. The pulse generator also provides an external sync signal for the Tektronix Model 545 scope, which has a Tektronix Model 1A7A 10- μ V sensitivity differential plug-in amplifier.

The modulated laser beam is passed through a sapphire prism before beam-splitting to eliminate the weak horizontally polarized beam from the

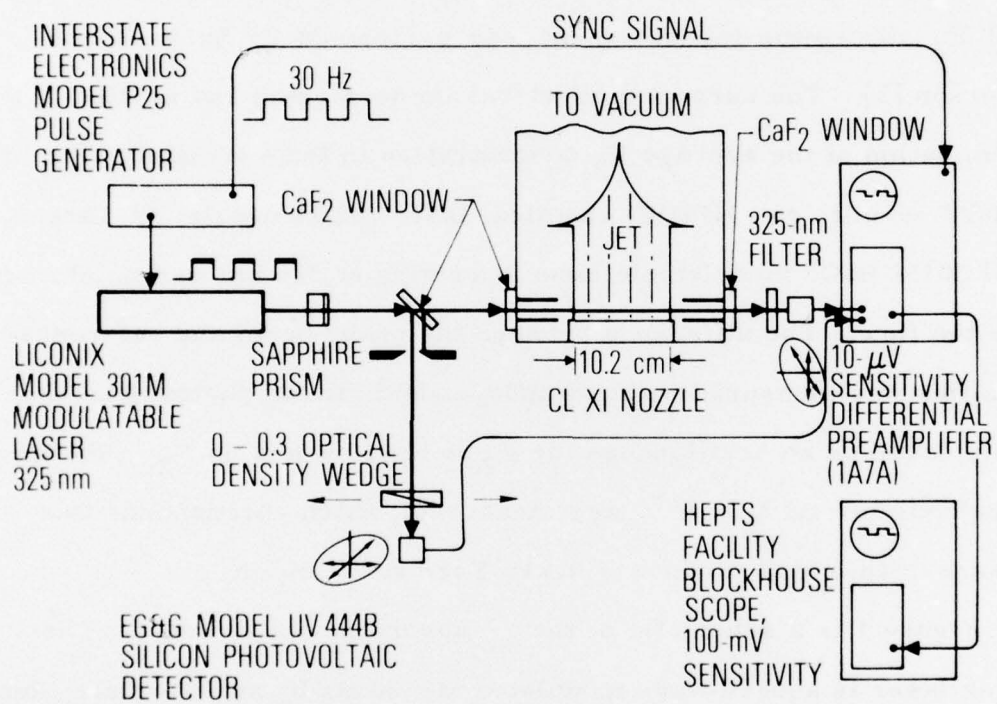


Fig. 1. Sensitive F₂ absorption experiment schematic

optical path, which otherwise produces differential transient noise signals because of the differences in laser turn-on and turn-off times and beam-splitter reflectivities and transmissivities, or both, relative to the vertically polarized beam. The beam splitter is a 6.25-mm-thick CaF_2 flat oriented at ~ 45 deg to the optical path. A thick flat (or wedge) is used as a beam splitter to eliminate one of the reflected beams to avoid noise generated from interference effects in the reference-beam detector. Orientation of the flat at ~ 45 deg results in a $\sim 15\%$ reflection of the S polarized beam from one surface of the flat. The 85% transmitted probe beam is attenuated to about this level by transmission through windows containing the absorption measurement region and (principally) through transmission through a narrow band optical filter centered at 325-nm wavelength ($T \sim 16\%$). The reference beam also passes through a quartz, linear optical density wedge of opacity range 0 to 0.3. Translation of this optical density wedge transverse to the optical path allows refined intensity variation of the reference beam to bring the two beams, as measured on the two EG&G Model UV 444B silicon photovoltaic detectors, into a condition of zero differential signal.

The detectors were connected to the differential input jacks of the Tektronix Model 1A7A 10- μV differential amplifier and were shunted by 1000- Ω load resistors. These load resistors maintained photovoltaic operation in the linear region of the characteristic curve. The detector radiation power sensitivity is nominally of constant value (within $\sim 2\%$) over

the entire detector surface. The peak-sensitivity surface positions of the detectors were easily determined by means of the sensitive differential arrangement employed here.

It was necessary to provide the detectors with translation capability in the two directions transverse to the beams to tune the beams to the peak-sensitivity spots. This procedure was essential for achieving measurement stability because beam jitter on the sides of the peak would result in the generation of differentially uncompensated signals. However, with both detectors peaked, signal changes resulting from beam jitter were minimized to an acceptable level.

Oscilloscope presentations of the laboratory data obtained with the system are shown in Figs. 2(a), 2(b), 2(c), and 2(d). Chopping frequency for these traces is nominally 18 Hz for each case. The reference (-B) and probe (A) signals as viewed independently on the scope (they are shown here in superposition) are shown in Fig. 2(a). The signal level, corresponding to I_0 , is 12 mV and is displayed on either side of the zero (no light) level. Note the absence of any transient effects at the instants of chopping, either on or off. The top trace of Fig. 2(b) is the -B trace alone with a reduced amplifier frequency bandpass (0 to 1 kHz), relative to the Fig. 2(a) display (0 to 1 MHz). Simultaneous display of the balanced A - B signals results in the middle trace in Fig. 2(b). These two traces are observed at a 10-mV/cm differential gain. The bottom trace in this figure is displayed at a gain three orders of magnitude smaller than the two top

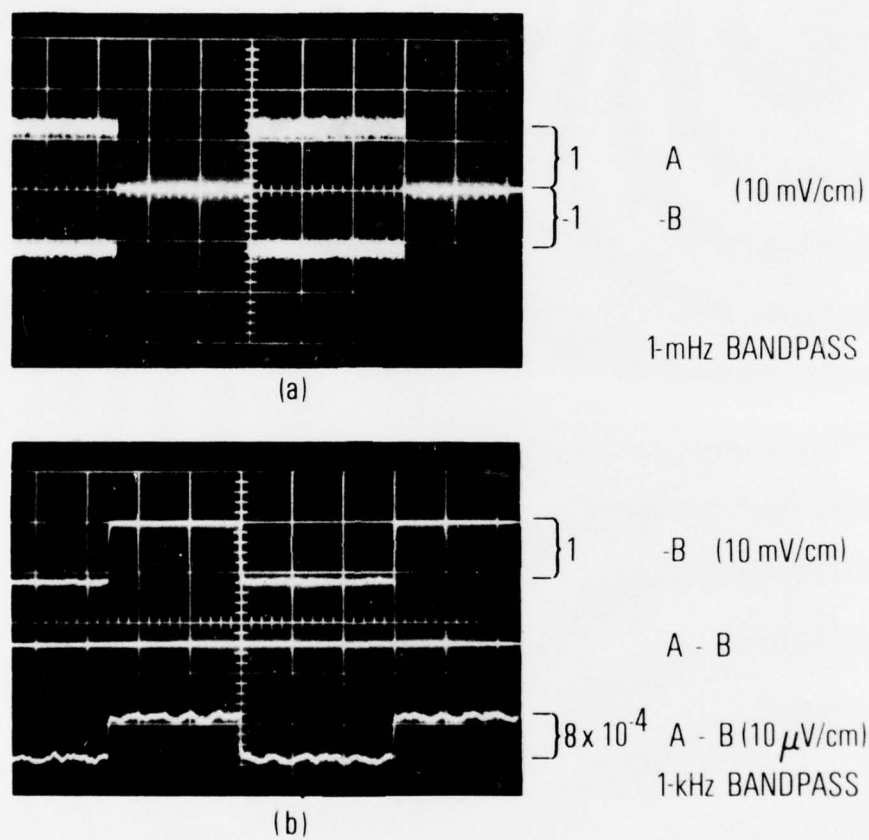


Fig. 2. F₂ absorption device scope traces. (a) and (b).

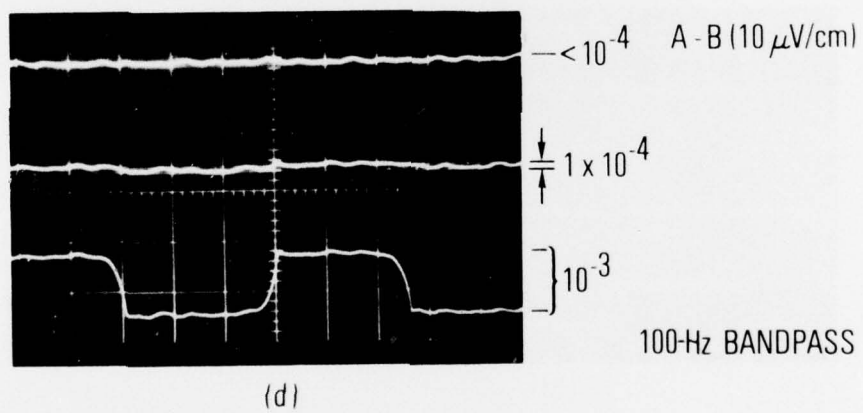
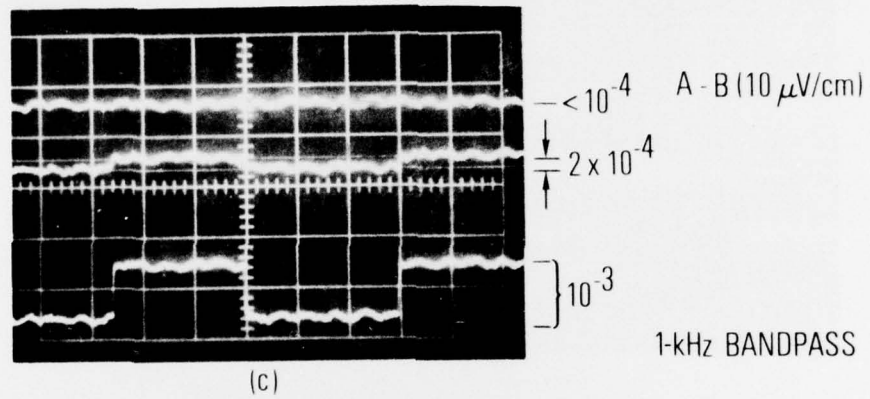


Fig. 2. F2 absorption device scope traces. (c) and (d).

traces (i. e. , $10 \mu\text{V}/\text{cm}$), where the previously unobservable imbalance of $\sim 9 \mu\text{V}$ ($\Delta I/I_0 = 8 \times 10^{-4}$) is seen. Further refinements in signal presentation are shown in Figs. 2(c) and (d). Figure 2(d) was obtained with the amplifier bandpass reduced to 100 Hz. A lower limit sensitivity of 1 part in 10^4 is shown in the central trace.

III. CALIBRATION

The F_2 continuum absorption coefficient at 325 nm (8.70 liter/mole cm) is obtained for 298 K by interpolation of the data obtained by Steunenberg and Vogel [6]. The temperature effect on the F_2 absorption coefficient for the F_2 continuum has been calculated by Hofland [7] and is presented in Fig. 3 in terms of absorption coefficient versus temperature for the 325-nm wavelength HeCd laser. There is a nearly constant temperature dependence over the temperature range of interest up to ~ 700 K and a maximum reduction of $\sim 15\%$ at 1500 K.

The F_2 absorption diagnostic was calibrated directly in an F_2 cold-flow facility. F_2 density along a path length between windows was determined by introducing F_2 in an N_2 diluent at known partial pressures into the flowing measurement chamber while monitoring steady-state chamber pressure and temperature. A flowing system was used to ensure against F_2 wall loss effects. Excellent agreement (within $\pm 2\%$) was obtained over the range $\Delta I/I_0 = 8 \times 10^{-4}$ to 2.9×10^{-2} between the measured absorption and the calculated absorption based upon the measured fluorine density (Fig. 4).

PRECEDING PAGE BLANK-NOT FILMED

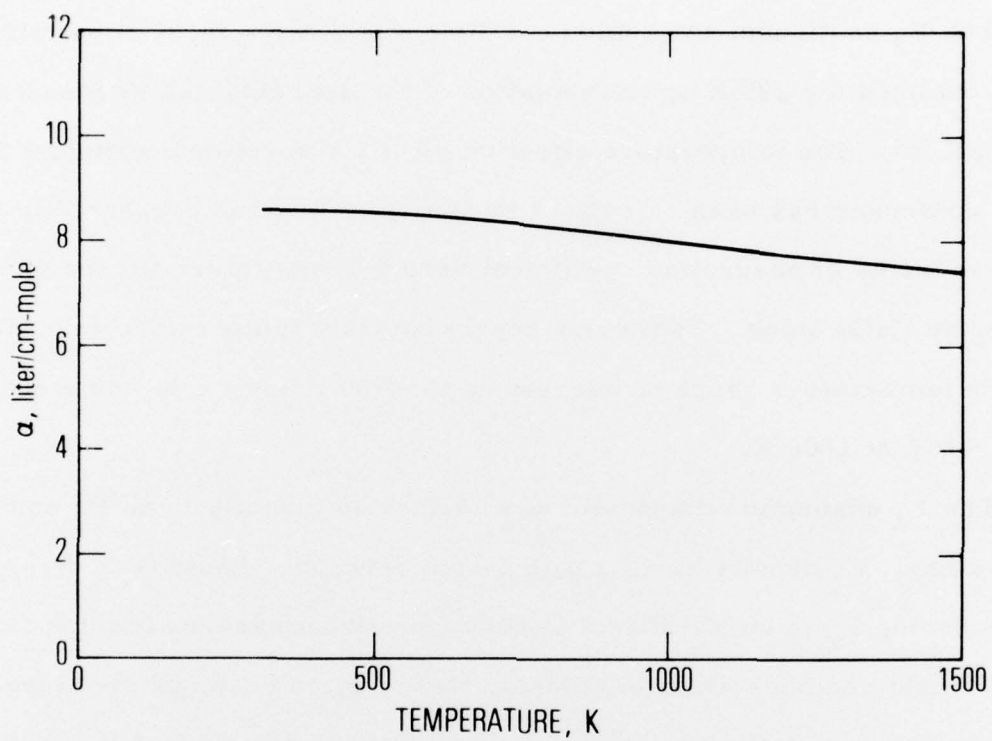


Fig. 3. Theoretical calculation of temperature effect on F_2 continuum absorption coefficient at 325 nm

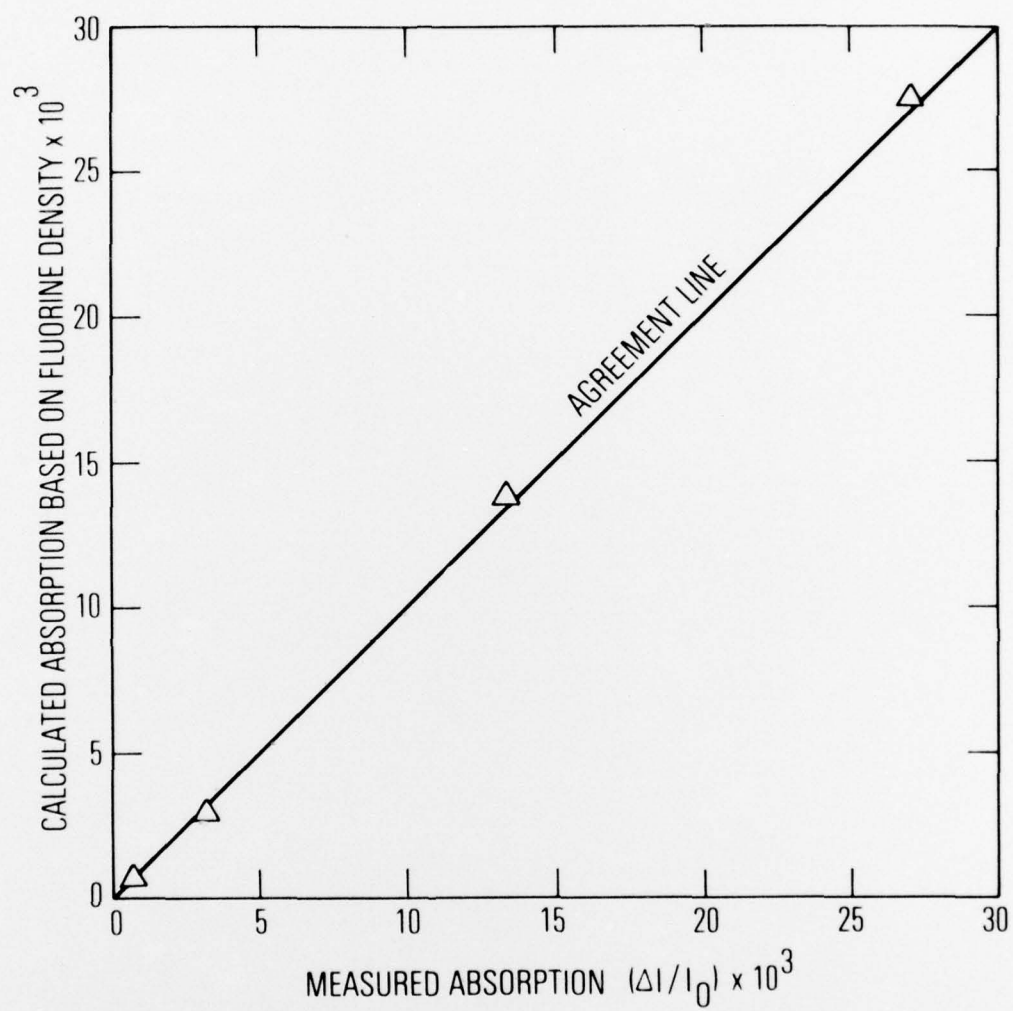


Fig. 4. F_2 absorption calibration in cold flow facility

IV. EXPERIMENTAL RESULTS

Hot-flow F_2 absorption measurements were made by means of the sensitive F_2 absorption diagnostic device in an Aerospace arc-heated, cw chemical laser facility. The probe laser beam was positioned 20 mm downstream of the nozzle exit plane along the jet centerline across the long dimension of the jet (17.8 cm). At this axial location, the jet static pressure closely approximates the more readily measurable cavity pressure. The nozzle employed was a standard 36-slit MESA nozzle [8]. CaF_2 windows were used for probe laser-beam transmission. The measurement was made initially for the cold flow to check the agreement with the calibration and for verification of the experimental setup.

The absorption equation for this experiment can be expressed as

$$\left(1 - \frac{\Delta I}{I_0}\right) = \exp \left[-8.70 \rho_{F_2} \text{ (mole/liter)} \right] \times 17.8 \text{ (cm)} \quad (1)$$

Measurement of $\Delta I/I_0$ allows determination of ρ_{F_2} , the fluorine molar density along the probe beam in the cavity. The molar fluorine density in the cavity may also be calculated for an assumed isentropic expansion from the plenum by means of the equations

$$\rho_{F_2} = \left(\frac{\dot{n}_{F_2}}{\dot{n}_{\text{total}}} \right) \rho_c \quad (2)$$

PRECEDING PAGE BLANK-NOT FILMED

$$\rho_c = \rho_t \left(\frac{p_c}{p_t} \right)^{1/\gamma} \quad (3)$$

and

$$\rho_t = \frac{p_t}{RT_t} \quad (4)$$

where ρ , p , and T are the gas density, pressure, and temperature, respectively; subscript t refers to plenum (total) conditions; subscript c refers to cavity conditions; R is the gas constant; $\gamma = c_p/c_v$; and \dot{n} is the molar flow rate.

The known mass flows of F_2 and He diluent gas and measured cavity and plenum pressures allow the calculation to be made. The He diluent molar flow was 100 times the F_2 flow in these tests. Hence, $\gamma = 1.67$ was employed here. For the cold-flow tests, $T_t = 300$ K.

For hot flow conditions, the plenum temperature was calculated by means of the pressure ratio method, i. e.,

$$T_{t_{\text{Hot}}} = T_{t_{\text{Cold}}} \left(\frac{p_{t_{\text{Hot}}}}{p_{t_{\text{Cold}}}} \right)^2 \quad (5)$$

for constant mass-flow conditions. A fictitious cavity molar fluorine density in a hot flow (ρ_{F_2}) was then calculated with no dissociation assumed in the plenum. Division of the measured F_2 density by the fictitious F_2 density,

where no dissociation was assumed to have taken place, results in a convenient normalization for data presentation, i.e., $\rho_{F_2 \text{ measured}} / \rho_{F_2 t} = 1 - \alpha$, where α is the standard dissociation level defined variously by

$$\alpha = \frac{\dot{m}_F}{\dot{m}_F + \dot{m}_{F_2}} = \frac{\dot{n}_F}{\dot{n}_F + 2\dot{n}_{F_2}} = \frac{\dot{n}_{F_2 t} - \dot{n}_{F_2 \text{ measured}}}{\dot{n}_{F_2 t}} \quad (6)$$

For the cold-flow case, $\rho_{F_2} = \rho_{F_2 t}$.

Data for a test series are presented in Fig. 5 in terms of $1 - \alpha$ versus plenum temperature. Mass flows were maintained at $\dot{m}_{He} = 4.00$ g/sec and $\dot{m}_{F_2} = 0.445$ g/sec. The plenum pressure was 1 atm, and the cavity pressure was maintained at 10 Torr by means of downstream vernier throttling. The cold-flow measurement made at 300 K plenum temperature yielded a measured value corresponding to no dissociation, which is in agreement with expectations. As plenum temperature is increased to ~ 1000 K (at 1 atm pressure), the dissociation of molecular fluorine begins and by 1500 K is complete. The dissociation curve is included in the figure to illustrate the temperature range. Because of plenum temperature uncertainties, the test points were taken over a range of temperatures to ensure that the obscuring effects of incomplete plenum dissociation were eliminated. In the temperature region from 1500 to 1900 K, the dissociation level is low, i.e., $\alpha < 0.5$. In addition, the dissociation level is reduced with increased temperature, clear evidence

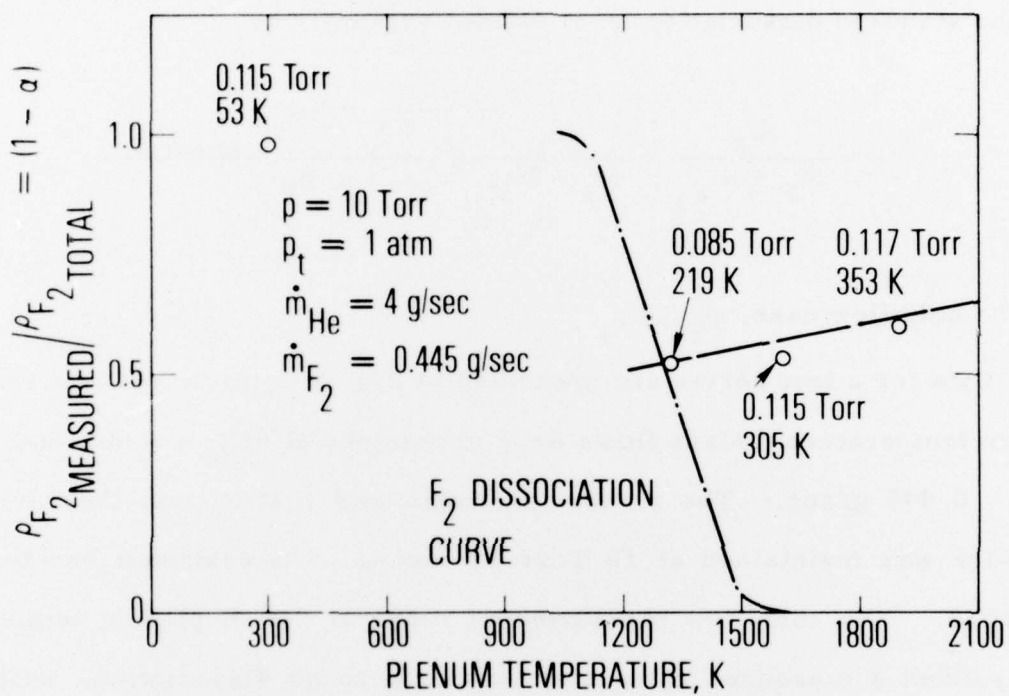


Fig. 5. F_2 density ratio measurement versus temperature

of strong recombination of the fluorine atoms in exhausting the nozzle. Gas-phase recombination yields only a fraction of this measured value; hence, the bulk of this recombination is expected to be the result of wall effects. The calculated cavity temperatures and F_2 partial pressures (average) are indicated near the room- and high-temperature experimental points for convenience.

A similar experiment was performed with SF_6 as the F_2 source. In this case, no cold-flow determination was possible; but hot-flow tests indicated the presence of F_2 (Fig. 6). The SF_6 flow indicated α to be 0.79 at 1500 K with a total possible molecular fluorine flow equal to three molecules F_2 per each SF_6 molecule assumed for purposes of normalization. This low value is certainly the result of incomplete plenum dissociation of the SF_6 . At a higher temperature, 2100 K, the measured α is ~ 0.45 , more nearly consistent with the F_2 flow measurements. Determination of F-atom concentration from this SF_6 measurement is, of course, much less straightforward than from the F_2 measurements.

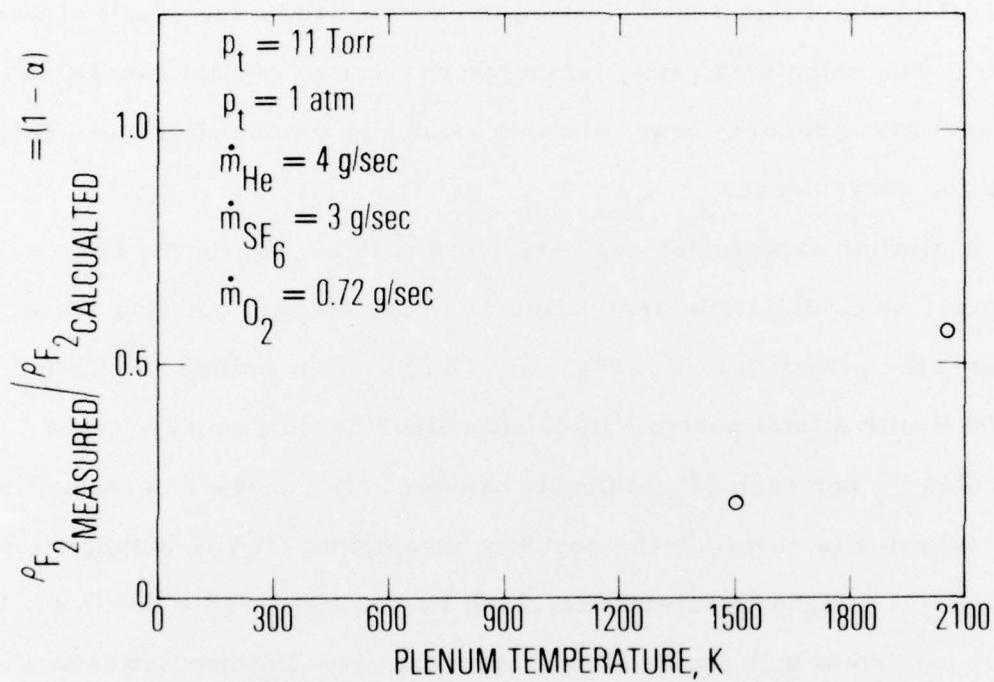


Fig. 6. F_2 absorption measurements in SF_6 flow

V. CONCLUDING REMARKS

A technique was developed to measure low-level F_2 concentrations by means of a difference absorption measurement with sensitivity $\Delta I/I_0 = 10^{-4}$, corresponding to a F_2 -pressure path length product of 0.215 Torr cm at 300 K. The diagnostic was applied to a hot-flow chemical laser and indicates that a rather high recombination in the nozzle flows, $\alpha = 0.4$ to 0.5, exists. Wall recombination in this chemical-laser nozzle may have had a dominant influence in determining F-atom concentrations in all HF (DF) chemical lasers in which this nozzle is used.

REFERENCES

1. D. J. Spencer, H. Mirels, and T. A. Jacobs, "Initial Performance of a CW Chemical Laser," *Opto-Electronics*, vol. 2, pp. 155-160, 1970.
2. W. S. King and H. Mirels, "Numerical Study of a Diffusion-Type Chemical Laser," AIAA Paper No. 72-146, presented at 10th Aerospace Sciences Meeting, San Diego, California, 17-19 January 1972.
3. H. Mirels and S. W. Liu, Boundary Layer Effects in Chemical Laser Nozzle Inlet, The Aerospace Corporation, to be published.
4. E. Jumper, "A Model for Fluorine Recombination at a Metal Surface," Dissertation, DS/ME/75-2, Air Force Institute of Technology (1975).
5. S. N. Suchard and L. D. Bergerson, "Fluorine Pressure Change Monitor for Reacting System," *The Review of Scientific Instruments*, vol. 43, no. 11, p. 1717, 1972.
6. R. K. Steunenberg and R. C. Vogel, "The Absorption Spectrum of Fluorine," J. Amer. Chem. Soc., vol. 78, p. 901, 1956.
7. R. Hofland, M. L. Lundquist, A. Ching, G. E. Thornton, and J. S. Whittier, "Dissociation Efficiency of Electron-Beam-Triggered Discharges for Initiating Atmospheric-Pressure H_2 - F_2 Lasers," AIAA Paper No. 75-848, presented at AIAA 8th Fluid and Plasma Dynamics Conference, Hartford, Connecticut, 16-18 June 1975.

8. H. Mirels and D. J. Spencer, "Power and Efficiency of a Continuous HF Chemical Laser," IEEE J. Quantum Electron, vol. QE-7, no. 11, pp. 501-507, 1971.

THE IVAN A. GETTING LABORATORIES

The Laboratory Operations of The Aerospace Corporation is conducting experimental and theoretical investigations necessary for the evaluation and application of scientific advances to new military concepts and systems. Versatility and flexibility have been developed to a high degree by the laboratory personnel in dealing with the many problems encountered in the nation's rapidly developing space and missile systems. Expertise in the latest scientific developments is vital to the accomplishment of tasks related to these problems. The laboratories that contribute to this research are:

Aerophysics Laboratory: Launch and reentry aerodynamics, heat transfer, reentry physics, chemical kinetics, structural mechanics, flight dynamics, atmospheric pollution, and high-power gas lasers.

Chemistry and Physics Laboratory: Atmospheric reactions and atmospheric optics, chemical reactions in polluted atmospheres, chemical reactions of excited species in rocket plumes, chemical thermodynamics, plasma and laser-induced reactions, laser chemistry, propulsion chemistry, space vacuum and radiation effects on materials, lubrication and surface phenomena, photo-sensitive materials and sensors, high precision laser ranging, and the application of physics and chemistry to problems of law enforcement and biomedicine.

Electronics Research Laboratory: Electromagnetic theory, devices, and propagation phenomena, including plasma electromagnetics; quantum electronics, lasers, and electro-optics; communication sciences, applied electronics, semiconducting, superconducting, and crystal device physics, optical and acoustical imaging, atmospheric pollution; millimeter wave and far-infrared technology.

Materials Sciences Laboratory: Development of new materials; metal matrix composites and new forms of carbon; test and evaluation of graphite and ceramics in reentry; spacecraft materials and electronic components in nuclear weapons environment; application of fracture mechanics to stress corrosion and fatigue-induced fractures in structural metals.

Space Sciences Laboratory: Atmospheric and ionospheric physics, radiation from the atmosphere, density and composition of the atmosphere, aurorae and airglow; magnetospheric physics, cosmic rays, generation and propagation of plasma waves in the magnetosphere; solar physics, studies of solar magnetic fields; space astronomy, x-ray astronomy; the effects of nuclear explosions, magnetic storms, and solar activity on the earth's atmosphere, ionosphere, and magnetosphere; the effects of optical, electromagnetic, and particulate radiations in space on space systems.

THE AEROSPACE CORPORATION
El Segundo, California